Microstructure and optical properties of Pr3+-doped hafnium silicate films

Yong-Tao An, Christophe Labbé, Larysa Khomenkova, Mag Morales, Xavier Portier, Fabrice Gourbilleau

Nanoscale Research Letters
a SpringerOpen Journal

NANO EXPRESS Open Access

Microstructure and optical properties of Pr^{3+}-doped hafnium silicate films

YongTao An, Christophe Labbé*, Larysa Khomenkova, Magali Morales, Xavier Portier and Fabrice Gourbilleau

Abstract

In this study, we report on the evolution of the microstructure and photoluminescence properties of Pr^{3+}-doped hafnium silicate thin films as a function of annealing temperature (T_A). The composition and microstructure of the films were characterized by means of Rutherford backscattering spectrometry, spectroscopic ellipsometry, Fourier transform infrared absorption, and X-ray diffraction, while the emission properties have been studied by means of photoluminescence (PL) and PL excitation (PLE) spectroscopies. It was observed that a post-annealing treatment favors the phase separation in hafnium silicate matrix being more evident at 950°C. The HfO_2 phase demonstrates a pronounced crystallization in tetragonal phase upon 950°C annealing. Pr^{3+} emission appeared at T_A = 950°C, and the highest efficiency of Pr^{3+} ion emission was detected upon a thermal treatment at 1,000°C. Analysis of the PLE spectra reveals an efficient energy transfer from matrix defects towards Pr^{3+} ions. It is considered that oxygen vacancies act as effective Pr^{3+} sensitizer. Finally, a PL study of undoped HfO_2 and $HfSiO_x$ matrices is performed to evidence the energy transfer.

Keywords: Praseodymium, Hafnium silicate, Oxygen vacancies, Photoluminescence, Energy transfer

Background

Rare-earth elements are important optical activators for luminescent devices. Among various rare-earth luminescent centers, trivalent praseodymium (Pr^{3+}) offers simultaneously a strong emission in the blue, green, orange, and red spectral range, satisfying the complementary color relationship [1,2]. Consequently, Pr^{3+}-doped glass/crystals are often used as phosphor materials [2,3]. SiO_2-(Ca, Zn)TiO_3:Pr^{3+} phosphors prepared with nanosized silica particles exhibit an intense red photoluminescence (PL) [3]. The Pr^{3+} emission was achieved for Si-rich SiO_2 (SRSO) implanted with Pr^{3+} ions, but its intensity was lower [4].

Hafnium dioxide (HfO_2) and hafnium silicates ($HfSiO_x$) are currently considered as the predominant high-*k* dielectric candidates to replace the conventional SiO_2 due to the rapid downscaling of the complementary metal-oxide semiconductor (CMOS) transistors [5,6]. It is ascribable to their good thermal stability in contact with Si, large electronic bandgaps, reasonable conduction band offset in regard to Si, and their compatibility with the current CMOS technology. Our group has first explored the structural and thermal stability of HfO_2-based layers fabricated by radio frequency (RF) magnetron sputtering [7,8] and their nonvolatile memory application [9,10].

It is worth to note that both HfO_2 and $HfSiO_x$ matrices have lower phonon frequencies compared to those of SiO_2, and as a consequence, both are expected to be suitable hosts for rare-earth activators. Thus, PL properties have been investigated for the HfO_2 matrix doped with Tb^{3+} [11], Eu^{3+} [11,12], or Er^{3+} [12,13] and have been explained by the interaction of rare-earth ions with host defects. Recently, our group has demonstrated that an enhancement of Er^{3+} PL emission can be achieved for the Er-doped $HfSiO_x$ matrix in comparison with that of the Er-doped HfO_2 [14]. It was also observed that an energy transfer from the HfO_2 host defects towards Er^{3+} ions, whereas the existence of Si clusters allowed an enhancement of the Er^{3+} ion emission under longer-wavelength excitation. Consequently, the mechanism of the excitation process, when Si clusters and oxygen-deficient centers act as Er^{3+} sensitizers, has been proposed to explain an efficient rare-earth emission from Er-doped $HfSiO_x$ hosts [14] similar to that observed for the Er-doped SRSO materials [15].

* Correspondence: christophe.labbe@ensicaen.fr
CIMAP, UMR 6252 CNRS/CEA/Ensicaen/UCBN, 6 Boulevard Maréchal Juin, Caen, Cedex 4 14050, France

In this paper, we study the microstructure and optical properties of Pr-doped hafnium silicate films fabricated by magnetron sputtering versus annealing temperature. We demonstrate that an efficient Pr^{3+} light emission is achievable by tuning the annealing conditions. The excitation mechanism of Pr^{3+} ions is also discussed.

Methods

The films were deposited onto p-type (100) 250-μm-thick Si wafers by RF magnetron sputtering of a pure HfO_2 target topped by calibrated Si and Pr_6O_{11} chips. The growth was performed in pure argon plasma with an RF power density of 0.98 $W{\cdot}cm^{-2}$; the Si substrate temperature was kept at 25°C. After deposition, a post-annealing treatment was carried out under a nitrogen flow, at temperatures (T_A) varying from 800°C up to 1,100°C for 1 h.

The refractive index (n) (given always at 1.95 eV) and the film thicknesses were deduced from spectroscopic ellipsometry data. The chemical composition of the films was determined by Rutherford backscattering spectrometry (RBS) using a 1.5-MeV $^4He^+$ ion beam with a normal incidence and a scattering angle of 165°. The infrared absorption properties were investigated by means of a Nicolet Nexus (Thermo Fisher Scientific, Waltham, MA, USA) Fourier transform infrared (FTIR) spectroscopy at Brewster's incidence (65°) in the range of 500 to 4,000 cm^{-1}. X-ray diffraction (XRD) experiments were performed using a Philips Xpert MPD Pro device (PANalytical B.V., Almelo, The Netherlands) with CuKα radiation (λ = 1.5418 Å) at a fixed grazing angle incidence of 0.5°. Cross-sectional specimens were prepared by standard procedure involving grinding, dimpling, and Ar^+ ion beam thinning until electron transparency for their observation by transmission electron microscopy (TEM). The samples were observed using a FEG 2010 JEOL instrument, operated at 200 kV. The PL emission and PL excitation (PLE) measurements were carried out using a 450-W Xenon arc lamp as excitation source at room temperature corrected on spectral response with the help of a Jobin-Yvon Fluorolog spectrometer (HORIBA Jobin Yvon Inc., Edison, NJ, USA).

Results and discussion

Composition and structural characterizations

In this study, the chemical composition of the film $Hf_{0.24}Si_{0.20}O_{0.52}Pr_{0.05}$ was determined through the simulation of the corresponding RBS spectrum using the SIMNRA program (Figure 1). The RBS analysis shows that the as-deposited film cannot be considered as a matrix of SiO_2 and HfO_2 only, as this is usually assumed for hafnium silicates. In our case, we deal with a hafnium silicate matrix enriched with silicon as well as doped with Pr^{3+} ions.

The inset of Figure 1 displays the refractive index evolution upon annealing treatment between 800°C and 1,100°C. The uncertainty of the refractive index is 0.01. Nevertheless, it was notable that it decreased with T_A. In a previous study on as-deposited film, it was found that

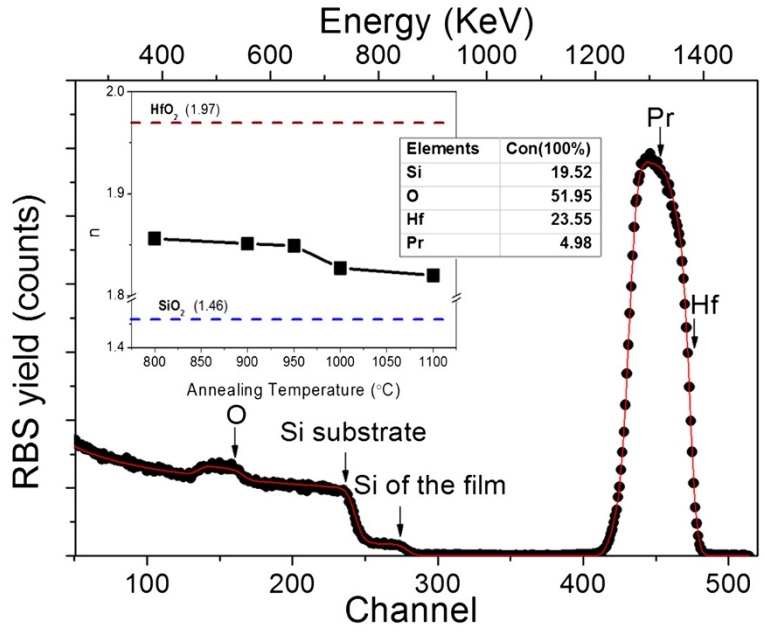

Figure 1 Experimental RBS spectrum (points) and simulated curve using SIMNRA (solid line) for as-deposited film. Inset table is the chemical composition of the film. Inset figure is the refractive index evolution versus T_A. The pure HfO_2 and pure SiO_2 indices are also shown in dashed lines. The films are about 170 nm in thickness.

the refractive index was about 2.2 [8], exceeding the value corresponding to the stoichiometric $HfSiO_4$ matrix (1.7) due to Si enrichment [8]. However, upon annealing, the refractive index is found to be about 1.85 (T_A = 800°C) and 1.82 (T_A = 1,100°C). If we exclude the decrease of porosity, this evolution could be explained by the increasing contribution of some phases with lower refractive index upon annealing (like SiO_2 (1.46)) [8].

Figure 2a represents the evolution of the FTIR spectra as a function of T_A. The FTIR spectrum of as-deposited film is represented by two broad vibration bands in the ranges of 500 to 750 and 800 to 1,200 cm^{-1}. An annealing treatment stimulates the appearance of several bands that peaked at about 827, 1,084, and 1,250 cm^{-1} (dashed lines in Figure 2a) corresponding to the LO_2-TO_2, TO_3, and LO_3 vibration modes of the Si-O bond, respectively. Moreover, the increase of the LO_3 mode intensity is attributed to the increase in the number of Si-O-Si bonds. This is a signature of the formation of the SiO_2 phase due to a phase separation process, leading to the decrease of the refractive index for $T_A \geq$ 800°C.

This phase separation is confirmed also by an increase of the vibration mode intensity in the range of 600 to 780 cm^{-1}, corresponding to Hf-O bonds for the formation of the HfO_2 phase [7,14]. The appearance of well-defined peaks at 760 and 660 cm^{-1} for $T_A \geq$ 1,050°C attests the presence of the monoclinic HfO_2 phase [16]. Besides, for $T_A \geq$ 1,050°C, two new absorption peaks that centered at 900 and 1,000 cm^{-1} appeared (detailed in Figure 2b). As we showed earlier [8], at such temperature, undoped $HfSiO_x$ did not reveal the presence of Si-O-Hf bonds. Thus, the vibration band at 900 and 1,000 cm^{-1} can be attributed to Si-O-Pr asymmetric mode. Similar incorporation of rare-earth ions into Si-O bonds and the formation of rare-earth silicate phase was observed earlier for SiO_x materials doped with Er^{3+}, Nd^{3+}, or $Pr^{3+}$and annealed at 1,100°C [17-19]. Thus, based on this comparison, one can conclude about the formation of Pr silicate revealed by FTIR spectra.

To get more information about the evolution of film structure, we performed XRD analyses. For as-deposited and 900°C annealed films, XRD spectra show a broad peak in the range of 25.0° to 35.0° with a maximum intensity located at $2\theta \approx 31.0°$ (Figure 3a). The shape of the XRD peak demonstrates the amorphous nature of both layers. With T_A increase, several defined peaks appear, emphasizing the formation of a crystalline structure. Thus, for T_A = 950°C, intense XRD peaks at $2\theta \approx 30.3°$, 35.0°, and 50.2° were detected. They correspond to the (111), (200), and (220) planes of the tetragonal HfO_2 phase, respectively, confirming the FTIR analysis [8]. The peak at $2\theta \approx 60.0°$ can be considered as an overlapping of the reflections from the (311) and (222) planes of the same HfO_2 phase. When T_A reaches 1,050°C, the appearance of peaks at almost $2\theta \approx 24.6°$ and 28.5° occurs. The first peak is attributed to the monoclinic HfO_2 phase (Joint Committee on Powder Diffraction Standards (JCPDS) no. 78–0050). The second one, at 28.5°, could be ascribed to several phases such as Pr_2O_3 ($2\theta_{[222]} \approx 27.699°$) (JCPDS no. 78–0309), Pr_6O_{11} ($2\theta_{[111]} \approx 28.26°$) (JCPDS no. 42–1121), Si ($2\theta_{[111]} \approx 28.44°$) (JCPDS no. 89–5012), or $Pr_2Si_2O_7$ ($2\theta_{[008]} \approx 29.0°$) (JCPDS no. 73–1154), due to the overlapping of corresponding XRD peaks. This observation is in agreement with the FTIR spectra (Figure 2b) showing the Hf-O vibrations and formation of Pr clusters.

In some oxygen-deficient oxide films [20,21], the phase separation is observed with the crystallization of the stoichiometric oxide matrix in the initial step and then in metallic nanoclustering. The aforesaid results are also coherent with our previous study of nonstoichiometric Hf-silicate materials in which we have evidenced the formation of HfO_2 and SiO_2 phases as well as Si

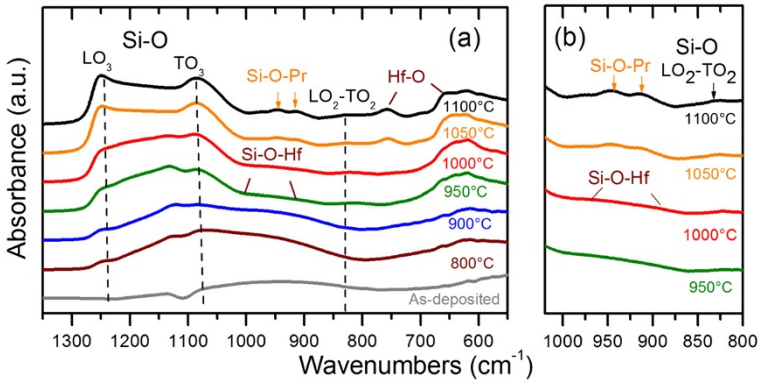

Figure 2 FTIR spectra of samples and detailed spectra between 800 and 1,020 cm^{-1}. (**a**) FTIR spectra of samples measured at Brewster's angle (65°) as a function of T_A for 1 h of nitrogen flow. Si-O bands are marked by dashed lines. (**b**) Detailed spectra between 800 and 1,020 cm^{-1} for better observation of the peak position in this range.

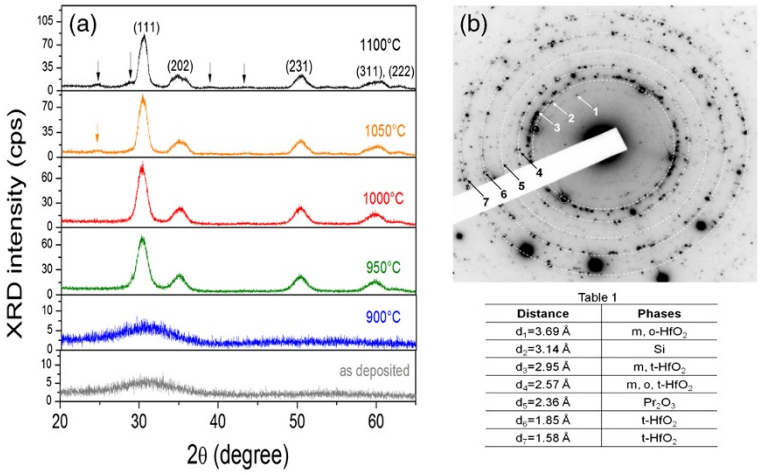

Table 1

Distance	Phases
d_1=3.69 Å	m, o-HfO_2
d_2=3.14 Å	Si
d_3=2.95 Å	m, t-HfO_2
d_4=2.57 Å	m, o, t-HfO_2
d_5=2.36 Å	Pr_2O_3
d_6=1.85 Å	t-HfO_2
d_7=1.58 Å	t-HfO_2

Figure 3 XRD and SAED patterns. (**a**) XRD patterns of as-deposited and annealed films. (**b**) SAED pattern of the 1,100°C-annealed film. Table one is the *d* spacing list obtained from (b) and the corresponding phases.

nanoclusters (Si-ncs) upon annealing treatment [14,22]. To underline this point, we performed a TEM observation of 1,100°C annealed sample and observed a formation of crystallized Si clusters. Figure 3b exhibits the corresponding selected area electron-diffraction (SAED) pattern. The analysis of dotted diffraction rings indicates the presence of several phases. Among them, one can see the signature of monoclinic and tetragonal HfO_2 phases, Pr_2O_3 phase, and crystallized Si phase (the Table one found in Figure 3b). This latter confirms the presence of Si-ncs but in a small amount (a few spots on the corresponding ring).

Photoluminescence properties

Figure 4a shows the PL spectra of Pr^{3+}-doped hafnium silicate films, which were excited by a 285-nm wavelength for Pr^{3+} ions. Remarkable emission is observed with peaks centered at about 475, 487, 503, 533, 595, 612, 623, 640, 667, 717, and 753 nm. They are associated to the Pr^{3+} energy level transitions $^3P_1 \rightarrow {}^3H_4$, $^3P_0 \rightarrow {}^3H_4$, $^3P_0 \rightarrow {}^3H_5$, $^1D_2 \rightarrow {}^3H_4$, $^3P_0 \rightarrow {}^3H_6$, $^3P_0 \rightarrow {}^3F_2$, $^3P_0 \rightarrow {}^3F_3$, and $^3P_0 \rightarrow {}^3F_4$, respectively, as shown in Figure 4b [23]. The maximum emission intensity corresponds to the peak centered at 487 nm due to the $^3P_0 \rightarrow {}^3H_4$ transition.

On the first step, the effect of annealing on Pr^{3+} PL properties was investigated (Figure 4c). The PL intensity evolution is shown in Figure 4d for the representative peak at 487 nm. The PL intensity increases with T_A rising from 800°C up to 1,000°C and then decreases with further T_A increase. At the initial stage, the annealing process is supposed to decrease the non-radiative recombination rates [24]. Thereafter, the quenching of the Pr^{3+} emission that occurred for T_A > 1,000°C can be due to the formation of the Pr^{3+} silicate or Pr oxide clusters (Figure 2) similar to the case observed in [17,18]. Moreover, it is interesting to note that the position of peak (Pr^{3+}: $^3P_0 \rightarrow {}^3H_4$) redshifts from 487 nm ($T_A \leq$ 1,000°C) to 492 nm (T_A = 1,100°C) as shown in Figure 4c. At the same time, two split peaks contributed to the $^1D_2 \rightarrow {}^3H_4$ transition that joined as one sharp peak which centered at 617 nm. All these results can be explained by the dependence of Pr^{3+} PL parameters on the crystal field associated with the type of Pr^{3+} environment [25]. Furthermore, the Pr^{3+} surrounding has been influenced by the crystallization of the HfO_2 phase for films annealed at T_A > 1,000°C.

Taking into account the formation of Si-ncs in Pr-doped $HfSiO_x$ samples annealed at 1,100°C for 1 h, one can expect the appearance of a PL emission due to exciton recombination inside Si-ncs, which is usually observed in the 700- to 950-nm spectral range [17,18]. However, our study of these samples did not reveal the Si-nc PL emission. Two reasons can be mentioned. The first one is the low density of Si-ncs, confirmed by the SAED pattern (Figure 3b). The second one is the efficient energy transfer from the Si-ncs to Pr^{3+} ions. However, based on the comparison of energetic diagrams of Pr^{3+} ions and Si-ncs, we observed that the energy levels of Si-ncs and Pr^{3+} ions have no overlapping. Thus, the energy transfer from Si-ncs toward Pr^{3+} ions should be very weak, contrary to an efficient sensitizing of other rare-earth ions such as Er^{3+} or Nd^{3+} in SiO_x or $HfSiO_x$ matrices [23,24]. Thus, in the case of Pr-doped $HfSiO_x$ samples, Si-ncs do not seem to be a major actor for the energy transfer. Nevertheless, due to the low amount of Si-ncs, their PL signal is not detectable.

Thus, the second step of our investigation was to study the mechanism of Pr^{3+} energy transfer under the 285-nm excitation wavelength. The energy diagram of Pr^{3+} ions

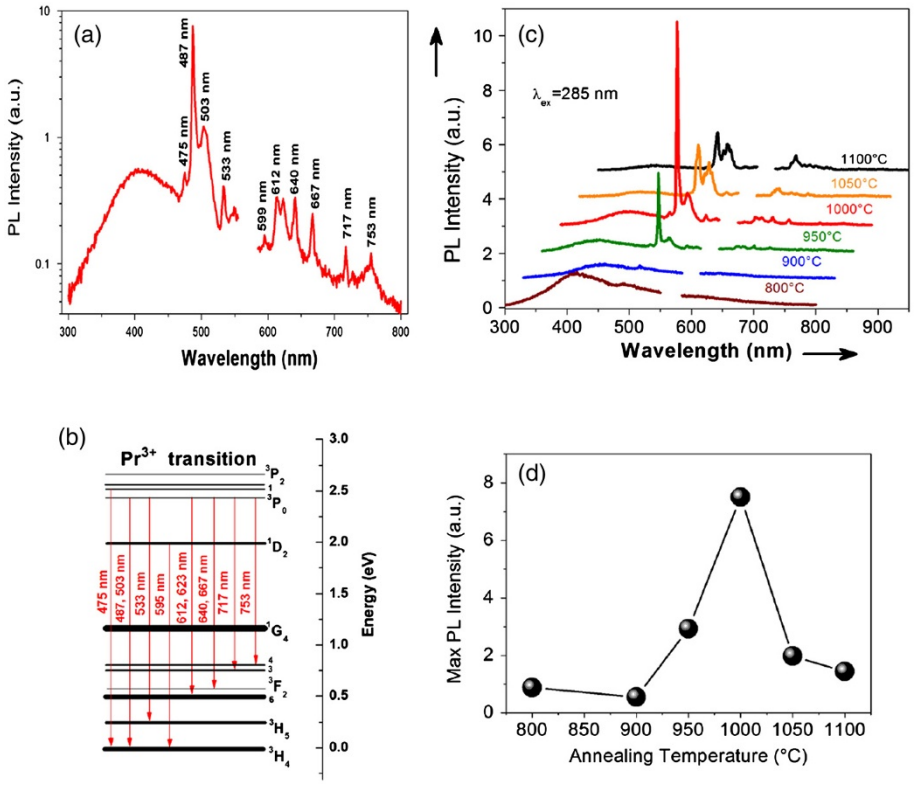

Figure 4 PL spectra, schematics, and PL behavior. (**a**) PL spectrum in logarithmic scale for 1,000°C annealed layer. (**b**) The schematics of the Pr^{3+} intra-4f transitions. (**c**) PL spectra of the films annealed at different annealing temperatures (T_A= 800°C to 1,100°C). The excitation wavelength is 285 nm. (**d**) The behavior of the PL intensity of the $^3P_0 \rightarrow {}^3H_4$ transition at 487 nm with T_A.

does not present such an absorption band wavelength at 285 nm (Figure 4b). In addition, the 4*f* to 5*d* transition is witted in upper energy level between 250 and 220 nm [26]. This evidences the indirect excitation of Pr^{3+} ions by the 285-nm wavelength and confirms an energy transfer behavior. To investigate this behavior in detail, we take interest in the strong background PL from 350 to 550 nm for the layers annealed at 800°C to 900°C in Figure 4c. This broad band may be ascribed to more than one kind of defect [5,6,27]. For the layers annealed at higher T_A such as 1,000°C, the intensity of this PL band drops deeply while the Pr^{3+} PL intensity increases notably. This suggests that the energy transfers from host defects to Pr^{3+} ions.

To understand this point, PLE spectra were recorded for the 'optimized' sample (annealed at 1,000°C) at different detection wavelengths (400, 487, and 640 nm, corresponding almost to the background emission for the former and to Pr^{3+} PL for the two latter), and they are presented in Figure 5. All the PLE spectra show a remarkable peak at about 280 nm (4.43 eV), and this peak position is in good agreement with that observed for oxygen vacancies [28]. According to some references [6,29], the O vacancies in the host matrix introduce a series of defect states (at about 1.85 to 4.45 eV) in the bandgap of HfO_2, which might provide recombination centers for excited *e* and *h* pairs. These excitons can effectively transfer energy to the nearby Pr^{3+} ions due to the overlapping with absorption levels of Pr^{3+} and, thus, to enhance the Pr^{3+} PL emission. Therefore, the Hf-related O vacancies in the host matrix serve as effective sensitizers to the adjacent Pr ions. An additional argument for this interaction is the increasing of Pr^{3+} PL intensity with T_A (from 900°C to 1,000°C) which caused the formation of HfO_2 grains, providing more Hf-related O vacancies. However, due to a decomposition process, formation of the Si-rich phase (Pr-doped SiO_x and/or Pr silicate) occurs too. The decrease of the intensity of the PL band that peaked at 400 nm and the increase of corresponding Pr^{3+} emission are a signature of the contribution of these Si-rich phase to the Pr^{3+} ion excitation (Figure 4c).

The excitation mechanism of Pr^{3+} ions was further explored by comparing two matrices. We carried out the PL experiments for three kinds of samples annealed at 1,000°C: undoped HfO_2, undoped $HfSiO_x$ films, and Pr-doped $HfSiO_x$ films excited by a 285-nm source (Figure 6). According to [6], in $HfSiO_x$ films, two types of O vacancies coexist: one is an O vacancy surrounded by

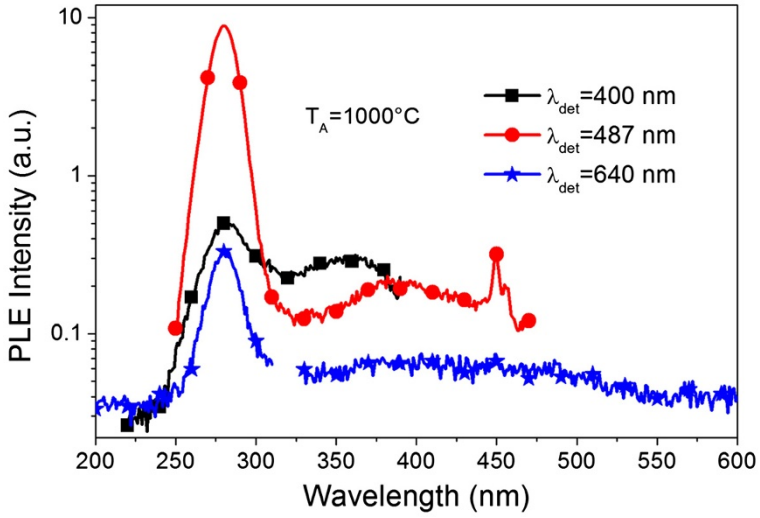

Figure 5 PLE spectra in logarithmic scale for 1,000°C annealed layer detected for different emission peaks.

Si atoms (Si-related O vacancy), while the other is an O vacancy surrounded by Hf atoms (Hf-related). Since the HfO_2 phase is ionic, it is obvious that it forms easier in the $HfSiO_x$ film upon annealing, and thus, Hf-related O vacancy formation is most preferable than Si-related O vacancy [6]. Herein, a particular interest is focused on the emissions from the defects: the Pr-doped film shows a broad band peaked at 420 nm, while the peak positions redshift to about 450 and 490 nm for $HfSiO_x$ and HfO_2 films, respectively. The 450-nm band can be fitted in energy into four Gaussian bands centered at 3.1, 2.84, 2.66, and 2.11 eV (table inset of Figure 6). The former two peaks are related to defects of the SiO_x phase, for instance, Si-related oxygen deficient centers [13,28]. The peak at 2.66 eV is ascribed to O vacancies related to the HfO_2 phase. The disappearance of the 2.66-eV PL component is accompanied with the appearance of the strong 487-nm emission and series of other Pr^{3+} transitions in Pr-doped $HfSiO_x$ film, which implies the energy transfer from O vacancies to the Pr sites.

As a result, the Si-rich HfO_2 host not only serves as a suitable matrix to achieve efficient Pr^{3+} emission, but

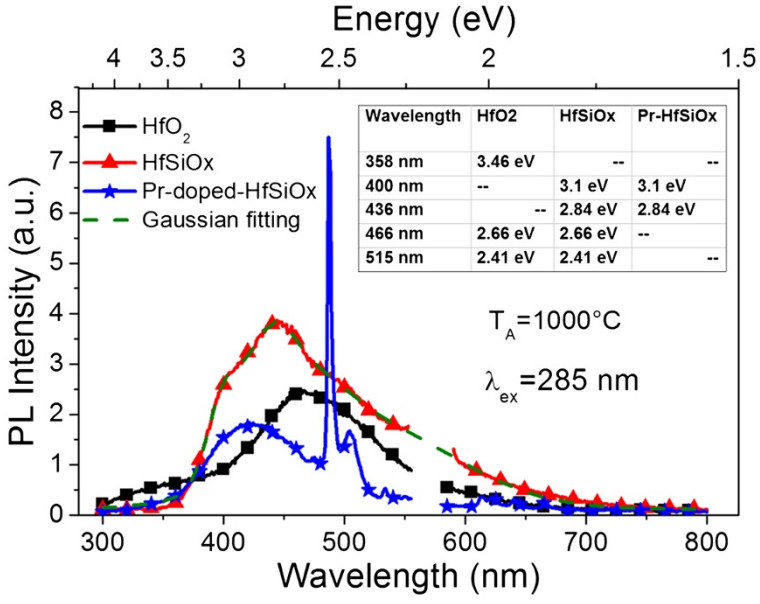

Wavelength	HfO2	HfSiOx	Pr-HfSiOx
358 nm	3.46 eV	--	--
400 nm	--	3.1 eV	3.1 eV
436 nm	--	2.84 eV	2.84 eV
466 nm	2.66 eV	2.66 eV	--
515 nm	2.41 eV	2.41 eV	--

Figure 6 PL spectra of Pr-doped and undoped $HfSiO_x$ and undoped pure HfO_2 films excited at 285 nm. The films were annealed at 1,000°C. Inset table is data of the fitting peaks.

also provides a sufficient amount of O vacancies acting as effective sensitizers of rare-earth ions.

Conclusions

In summary, we have fabricated the Pr^{3+}-doped hafnium silicate layers by RF magnetron sputtering. The effect of the annealing temperature on the film properties has been investigated by means of ellipsometry, XRD, and FTIR spectroscopies. We showed that the highest Pr^{3+} PL intensity is obtained for 1,000°C annealing. The PL and PLE measurements demonstrate that the Pr^{3+} ions were efficiently excited by oxygen vacancies in the films, and thus, remarkable Pr^{3+} PL can be obtained by a non-resonant excitation process. The present results show the promising application of Pr-doped films for future optoelectronic devices.

Competing interests

The authors declare that they have no competing interests.

Authors' contributions

YTA fabricated the Pr-doped layers, carried out the characterization studies, as well as wrote the draft of manuscript. LK fabricated the undoped layers. MM performed the RBS measurements and refinements. XP performed the TEM study. CL and FG coordinated the study. All authors discussed and commented on the manuscript. All authors read and approved the final manuscript.

Acknowledgments

The authors would like to thank Dr. Ian Vickridge from SAFIR, Institut des NanoSciences de Paris for the RBS data as well as Dr. Sophie Boudin from CRISMAT Lab for the measurement of PL and PLE spectra. This work is supported by the CEA/DSM/ENERGY contract (Project HOFELI) and the Chinese Scholarship Council (CSC) program.

Received: 9 October 2012 Accepted: 23 December 2012
Published: 21 January 2013

References

1. Birkhahn R, Garter M, Steckl AJ: **Red light emission by photoluminescence and electroluminescence from Pr-doped GaN on Si substrates.** *Appl Phys Lett* 1999, **74:**2161.
2. Wang W, Jiang C, Shen MR, Fang L, Zheng FG, Wu XL, Shen JC: **Effect of oxygen vacancies on the red emission of $SrTiO_3$:Pr^{3+}phosphor films.** *Appl Phys Lett* 2009, **94:**081904.
3. Haranath D, Khan AF, Chander H: **Luminescence enhancement of (Ca, Zn) TiO_3: Pr^{3+} phosphor using nanosized silica powder.** *Appl Phys Lett* 2006, **89:**091903.
4. Zhu F, Xiao ZS, Yan L, Zhang F, Zhong K, Cheng GA: **Photoluminescence and radiation effect of Er and Pr implanted silicon-rich silicon oxide thin films.** *Nucl Instr Meth Phys RES, Sect B* 2009, **267:**3100.
5. Choi JH, Mao Y, Chang JP: **Development of hafnium based high-*k* materials-a review.** *Mater Sci Eng, R* 2011, **72:**97.
6. He G, Zhu LQ, Sun ZQ, Wan Q, Zhang LD: **Integrations and challenges of novel high-*k* gate stacks in advanced CMOS technology.** *Prog Mater Sci* 2011, **56:**475.
7. Khomenkova L, Dufour C, Coulon PE, Bonafos C, Gourbilleau F: **High-*k* Hf-based layers grown by RF magnetron sputtering.** *Nanotechnology* 2010, **21:**095704.
8. Khomenkova L, Portier X, Cardin J, Gourbilleau F: **Thermal stability of high-*k* Si-rich HfO_2 layers grown by RF magnetron sputtering.** *Nanotechnology* 2010, **21:**285707.
9. Khomenkova L, Portier X, Sahu BS, Slaoui A, Bonafos C, Schamm-Chardon S, Carrada M, Gourbilleau F: **Silicon nanoclusters embedded into oxide host for non-volatile memory applications.** *ECS Trans* 2011, **35:**37.
10. Khomenkova L, Sahu BS, Slaoui A, Gourbilleau F: **Hf-based high-*k* materials for Si nanocrystal floating gate memories.** *Nanoscale Res Lett* 2011, **6:**172.
11. Liu LX, Ma ZW, Xie YZ, Su YR, Zhao HT, Zhou M, Zhou JY, Li J, Xie EQ: **Photoluminescence of rare earth^{3+} doped uniaxially aligned HfO_2 nanotubes prepared by sputtering with electrospun polyvinylpyrolidone nanofibers as templates.** *J Appl Phys* 2010, **107:**024309.
12. Lange S, Kiisk V, Aarik J, Kirm M, Sildos I: **Luminescence of ZrO_2 and HfO_2 thin films implanted with Eu and Er ions.** *Phys Stat sol (c)* 2007, **4:**938.
13. Wang JZ, Xia Y, Shi Y, Shi ZQ, Pu L, Zhang R, Zheng YD, Tao ZS, Lu F: **1.54 μm photoluminescence emission and oxygen vacancy as sensitizer in Er-doped HfO2 films.** *Appl Phys Lett* 2007, **91:**191115.
14. Khomenkova L, An YT, Labbé C, Portier X, Gourbilleau F: **Hafnia-based luminescent insulator for phosphor applications.** *ECS Trans* 2012, **45**(5):119.
15. Cueff S, Labbé C, Dierre B, Cardin J, Khomenkova L, Fabbri F, Sekiguchi T, Rizk R: **Cathodoluminescence and photoluminescence comparative study of Er-doped Si-rich silicon oxide.** *J Nanophotonics* 2011, **5:**051504.
16. Nguyen NV, Davydov AV, Chandler-Horowitz D, Frank MM: **Sub-bandgap defect states in polycrystalline hafnium oxide and their suppression by admixture of silicon.** *Appl Phys Lett* 2005, **87:**192903.
17. Talbot E, Lardé R, Pareige P, Khomenkova L, Hijazi K, Gourbilleau F: **Nanoscale evidence of erbium clustering in Er doped silicon rich silica.** *Nanoscale Res Lett*, . in press.
18. Debieu O, Bréard D, Podhorodecki A, Zatryb G, Misiewicz J, Labbé C, Cardin J, Gourbilleau F: **Effect of annealing and Nd concentration on the photoluminescence of Nd^{3+} ions coupled with silicon nanoparticles.** *J Appl Phys* 2010, **108:**113114.
19. Kukli K, Ritala M, Pilvi T, Sajavaara T, Leskela M, Jones AC, Aspinall HC, Gilmer DC, Tobin PJ: **Evaluation of a praseodymium precursor for atomic layer deposition of oxide dielectric films.** *Chem Mater* 2004, **16:**5162.
20. Perrière J, Hebert C, Petitmangin A, Portier X, Seiler W, Nistor M: **Formation of metallic nanoclusters in oxygen deficient indium tin oxide films.** *J Appl Phys* 2011, **109:**123704.
21. Millon E, Nistor M, Hebert C, Davila Y, Perrière J: **Phase separation in nanocomposite indium oxide thin films grown at room temperature: on the role of oxygen deficiency.** *J Mater Chem* 2012, **22:**12179.
22. Talbot E, Roussel M, Genevois C, Pareige P, Khomenkova L, Portier X, Gourbilleau F: **Atomic scale observation of phase separation and formation of silicon clusters in Hf high-*k* silicates.** *J Appl Phys* 2012, **111:**103519.
23. Maqbool M, Richardson HH, Kordesch ME: **Luminescence from praseodymium doped AlN thin films deposited by RF magnetron sputtering and the effect of material structure and thermal annealing on the luminescence.** *J Mater Sci* 2007, **42:**5657.
24. Polman A, Jacobson DC, Eaglesham DJ, Kistler RC, Poate JM: **Optical doping of waveguide materials by MeV Er implantation.** *J Appl Phys* 1991, **70:**3778.
25. Ramos-Brito F, Alejo-Armenta C, Garcia-Hipolito M, Camarillo E, Hernandez AJ, Murrieta SH, Falcony C: **Photoluminescence emission of Pr^{3+} ions in different zirconia crystalline forms.** *Opt Mater* 1840, **2008:**30.
26. van der Kolk E, Dorenbos P, van Eijk CWE: **Vacuum ultraviolet excitation and quantum splitting of Pr^{3+} in $LaZrF_7$ and α-$LaZr_3F_{15}$.** *Opt Commun* 2001, **197:**317.
27. Chen TJ, Kuo CL: **First principles study of the oxygen vacancy formation and the induced defect states in hafnium silicates.** *J Appl Phys* 2012, **111:**074106.
28. Wang JZ, Shi ZQ, Shi Y, Pu L, Pan LJ, Zhang R, Zheng YD, Tao ZS, Lu F: **Broad excitation of Er luminescence in Er-doped HfO_2 films.** *Appl Phys A* 2009, **94:**399.
29. Xiong K, Du Y, Tse K, Robertson J: **Defect states in the high-dielectric-constant gate oxide $HfSiO_4$.** *J Appl Phys* 2007, **101:**024101.

doi:10.1186/1556-276X-8-43
Cite this article as: An *et al.*: Microstructure and optical properties of Pr^{3+}-doped hafnium silicate films. *Nanoscale Research Letters* 2013 **8**:43.